# Optimal Third-Harmonic Current Injection for Asymmetrical Multiphase PMSMs

A. Cervone, *Student Member*, *IEEE*, M. Slunjski, *Student Member*, *IEEE*, E. Levi, *Fellow, IEEE*, G. Brando

***Abstract*—The paper proposes a modelling approach and an optimization strategy to exploit a third harmonic current injection for the torque enhancement in multiphase isotropic PMSMs with non-sinusoidal back-EMFs. The modelling approach is based on a proper vector space decomposition and on the associated rotational transformation, aimed to properly select a set of stator current space vectors to be controlled. It is presented for a generic (i.e. asymmetrical, with an arbitrary angular shift) winding configuration. The injection strategy is related to the choice of a constant synchronous current set, aimed at minimizing the average stator winding losses for a given reference torque by using the 1st and the 3rd spatial harmonics of the air-gap flux density. The optimal solution has been found analytically and has been developed in detail for a selected set of asymmetrical winding configurations. Both the numerical and experimental results are in good agreement with the theoretical analysis.**

***Index Terms*—Multiphase drives, surface mounted PMSM, asymmetrical machines, non-sinusoidal back-EMF, third-harmonic current injection, power loss minimization.**

## I. Introduction

Multiphase electrical machines represent a viable alternative to traditional three-phase ones in many high-power and high-reliability applications, ranging from wind energy generation to electrical traction (e.g. electric/hybrid vehicles, more electric aircraft, ship propulsion, etc.) [1-3]. Among the many benefits they offer, multiphase machines can continue to operate at reduced power even after multiple phase faults, as long as the healthy phases are able to produce a rotating air-gap flux-density field [1-3]. Moreover, for a given rated power and voltage, a multiphase machine's rated current is lower than in its three-phase counterpart, allowing to employ converters with reduced current ratings, thus leading to more reliable operation and higher efficiency [1]. Finally, the higher number of phases leads to additional degrees of freedom, which can be exploited for additional control purposes [1-7]. This includes independent utilization of different spatial harmonics of the air-gap flux density generated by the stator currents to enhance torque production [1-7].

For permanent magnet synchronous machines (PMSMs), this property can be exploited to increase the torque/current ratio by properly coupling the stator's and rotor's contribution for different viable spatial harmonics [4-7]. This approach leads to a set of non-sinusoidal currents in steady state conditions and, consequently, corresponds to a higher order current harmonic injection. In particular, when only the third-order spatial harmonic is exploited, a proper third harmonic injection strategy can be implemented [4-7]. In this case the optimization problem is reduced to the identification of the optimal ratio between the two stator-driven harmonic contributions to the air-gap flux density.

In the case of machines characterized by an odd number of phases and a symmetrical winding configuration, it has been verified that, based on the stator winding loss minimization criterion, the optimal injection ratio coincides with the one between the corresponding magnets' induced back-EMFs [4-13]. Several applications of these strategies can be found, especially for five-phase machines [9-17].

On the contrary, the higher-order harmonic injection for asymmetrical winding configurations has been rarely discussed in the literature, the exceptions being [18-22]. While [18] considers the 5th and the 7th harmonic injection, in [19] and [20-21] a third harmonic injection has been investigated for a six-phase induction machine and a six-phase PMSM, respectively. However, the torque enhancement requires connection of the winding's neutral point to either an additional inverter leg or to the midpoint of the capacitor bank in the dc link, to allow the free circulation of the injected harmonic. The third harmonic amplitude is equal in all phases.

As an alternative, in [22] the authors have shown how the torque enhancement can be applied in an asymmetrical nine-phase PMSM with a single but isolated neutral point. In this case the optimal injection ratio is modified with respect to the symmetrical configuration. This paper extends the results given in [22] by formulating the optimization problem with respect to a generic *n*-phase PMSM. The approach, by exploiting a proper vector space decomposition (VSD) and the associated rotational transformation, is able to highlight how each current component contributes to the electromagnetic torque and to the average power losses (Section II). Consequently, the generalized optimization problem can be formulated in a compact way; the solution can be found analytically and it only depends on the magnitude of the magnets' induced fluxes (responsible for the electromagnetic torque) and on the winding configuration (responsible for the power losses) (Section III).

The proposed strategy has been particularized for selected examples of machines with an asymmetrical winding configuration. (Section IV). Both a numerical and an experimental validation has also been performed employing a nine-phase asymmetrical machine (Section V). Section VI sums up the conclusions of the work.

Manuscript received November 12, 2019; revised January 27, 2020 and March 3, 2020; accepted March 8, 2020.

A. Cervone and G. Brando are with the Department of Electrical Engineering and Information Technology, University of Naples Federico II, 80125, Naples, Italy (e-mail: andrea.cervone@unina.it; gianluca.brando@unina.it)

M. Slunjski and E. Levi are with the Faculty of Engineering and Technology, Liverpool John Moores University, Liverpool L3 3AF, U.K. (e-mail: M.Slunjski@2017.ljmu.ac.uk; E.Levi@ljmu.ac.uk).

## II. Mathematical Model

The machine under analysis is assumed to have $n$ identical stator windings arranged in $P_p$ pole pairs and distributed along the machine's stator periphery so that their magnetic axes have an electrical phase displacement of $\alpha_k$ (with $k = 1, \ldots, n$) with respect to an arbitrary reference. The windings are assumed to be connected into a single neutral point and supplied by a voltage source inverter (VSI); the architecture is schematically represented in Fig. 1.

The magnetic flux density in the air-gap generated by the rotor's permanent magnets (PMs), once decomposed in a Fourier series with respect to the stator electric angle, is in general given by the superposition of an infinite number of spatial harmonics. These harmonics produce in each $k$-th stator winding a flux which can be expressed as:

$$\lambda_k(\theta) = \sum\nolimits_h \lambda_{Mh} \cos\left(h(\theta - \alpha_k) + \varphi_h\right) \tag{1}$$

where $\lambda_{Mh}$ and $\varphi_h$ are the magnitude and the phase displacement of the flux contribution due to the $h$-th flux density spatial harmonic, while $\theta$ denotes the electric angle between the rotor reference axis and the stator reference one.

### A. Per-phase Electrical Equations

Assuming linearity, the mathematical model of a magnetically isotropic PMSM with a single isolated neutral point (Fig. 1) is represented by the set of equations [1]:

$$\begin{cases} [u_{\text{ph}}] + v_{ON} \cdot [1_{n\times 1}] = [v_{\text{ph}}] = [R] \cdot [i_{\text{ph}}] + [L] \cdot \dfrac{\text{d}}{\text{d}t}[i_{\text{ph}}] + [e_{\text{ph}}] \\ [1_{n\times 1}]^{\text{T}} \cdot [i_{\text{ph}}] = \sum\nolimits_{k=1}^{n} i_k = 0 \end{cases} \tag{2}$$

where $[u_{\text{ph}}]$, $[e_{\text{ph}}]$ and $[i_{\text{ph}}]$ are the sets of the inverter's leg voltages, PM induced back-EMFs and stator winding currents, $v_{ON}$ is the voltage between the inverter's dc link mid-point $O$ and the machine's neutral point $N$, $[v_{\text{ph}}]$ is the set of the stator winding voltages, $[R]$ is the winding resistances matrix ($[R] = R \cdot [I_{n\times n}]$), $[L]$ is the stator winding inductance matrix (which includes both the mutual and the leakage contributions), and $[1_{n\times 1}] = [1,1,\ldots,1]^{\text{T}}$ is the unitary $n\times 1$ column vector.

The PM induced back-EMFs are expressed as:

$$e_k = \frac{\text{d}\lambda_k}{\text{d}t} = \omega \cdot \frac{\partial \lambda_k}{\partial \theta} = -\omega \cdot \sum\nolimits_h h \cdot \lambda_{Mh} \sin\left(h(\theta - \alpha_k) + \varphi_h\right) \tag{3}$$

where $\omega = \text{d}\theta/\text{d}t$ is the machine's rotor electrical speed.

### B. Torque Expression in the Space Vector Formalism

By applying a set of currents to the machine's stator windings, the magnetic flux density in the air-gap is modified. This new current-dependent field can be once again decomposed in an infinite number of spatial harmonics, each of which can be identified through an $h$-th order space vector:

$$\mathbf{i}_h = i_{\text{x}h} + \text{j} \cdot i_{\text{y}h} = \sqrt{2/n} \cdot \sum\nolimits_{k=1}^{n} i_k \cdot \text{e}^{\text{j}h\alpha_k} \tag{4}$$

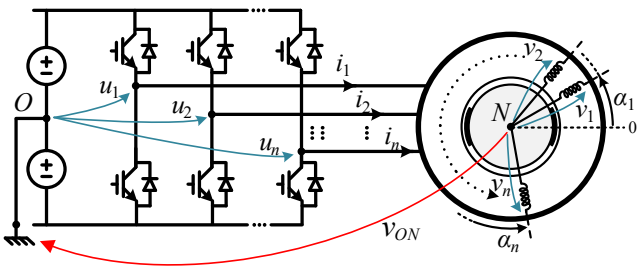


Fig. 1. System architecture for an $n$-phase PMSM with a single neutral point.

By expressing each space vector $\mathbf{i}_h$ in a $h$-th spatial harmonic synchronous reference frame through the complex rotation:

$$\mathbf{i}_h^{\langle \text{dq} \rangle} = i_{\text{d}h} + \text{j} \cdot i_{\text{q}h} = \mathbf{i}_h \cdot \text{e}^{-\text{j}(h\theta + \varphi_h)} \tag{5}$$

and by considering (1), the electromagnetic torque developed by the PMSM can be analytically expressed as:

$$\begin{aligned} T_{em} &= P_p \cdot \sum\nolimits_{k=1}^{n} i_k \cdot (\partial \lambda_k / \partial \theta) = \\ &= P_p \cdot \sum\nolimits_h h \cdot \lambda_{Mh} \cdot \left[ \sum\nolimits_{k=1}^{n} i_k \cdot \sin\left(h(\theta - \alpha_k) + \varphi_h\right) \right] = \\ &= P_p \cdot \sum\nolimits_h h \cdot \lambda_{Mh} \cdot \left[ \sqrt{n/2} \cdot \text{Im}\left\{ \mathbf{i}_h \cdot \text{e}^{-\text{j}(h\theta + \varphi_h)} \right\} \right] = \\ &= \sum\nolimits_h \left( P_p \cdot \sqrt{n/2} \cdot h \cdot \lambda_{Mh} \right) \cdot i_{\text{q}h} = \sum\nolimits_h \kappa_h \cdot i_{\text{q}h} \end{aligned} \tag{6}$$

where $\kappa_h = P_p \cdot \sqrt{n/2} \cdot h \cdot \lambda_{Mh}$ is a constant gain related to the $h$-th harmonic. Only the quadrature components of the space vectors, by interacting with the corresponding harmonics of the PM induced fluxes, are responsible for the torque production. However, it is important to observe that, since the phase currents form an $n$-dimensional set, only up to $n$ scalar components of the space vectors can be set arbitrarily.

Moreover, the winding configuration further reduces the number of controllable components by forcing to zero the sum of all the phase currents (second equation in (2)): this condition can be conveniently expressed in terms of a zero-sequence component constraint as $i_0 = (\sum_{k=1}^{n} i_k)/\sqrt{n} = 0$.

### C. Choice of the VSD Transformation

As for standard multiphase machines, the mathematical model can be reformulated through a variable transformation known as Vector Space Decomposition (VSD) [1-3]. The transformed current set $[i_{\text{VSD}}]$ should be chosen in order to include a set of space vector components $\{i_{\text{x}h}, i_{\text{y}h}\}$ to be controlled and the zero-sequence component $i_0$ (constrained to zero by hardware configuration). The correlation between the transformed current set $[i_{\text{VSD}}]$ and the phase current set $[i_{\text{ph}}]$ is:

$$[i_{\text{VSD}}] = [\text{C}] \cdot [i_{\text{ph}}] \quad \Leftrightarrow \quad [i_{\text{ph}}] = [\text{T}] \cdot [i_{\text{VSD}}] \tag{7}$$

with $[\text{C}]$ the generalized Clarke's transformation matrix.

As per (4), the components of each $h$-th space vector $\mathbf{i}_h$ can be introduced into $[i_{\text{VSD}}]$ through the set of rows:

$$[\text{C}_h] = \sqrt{\frac{2}{n}} \cdot \begin{bmatrix} \cos(h\alpha_1) & \cos(h\alpha_2) & \cdots & \cdots \\ \sin(h\alpha_1) & \sin(h\alpha_2) & \cdots & \cdots \end{bmatrix} \tag{8}$$

while $i_0$ can be introduced through the row $[\text{C}_0] = [1_{n\times 1}]^{\text{T}}/\sqrt{n}$.

Obviously, $[\text{C}]$ needs to be a full rank matrix to guarantee the existence of its inverse $[\text{T}] = [\text{C}]^{-1}$ and, therefore, preserve the number of state variables. As a result, a chosen set of space vectors can be controlled only if the corresponding rows in the transformation matrix are linearly independent from each other. For an odd number of phases it is possible to control at most $(n-1)/2$ space vectors at the same time, while, for an even number of phases, the number of independently controllable space vectors is $(n-2)/2$: in this case, to get a full-rank transformation matrix, after introducing the corresponding $(n-2)$ rows as per (8) and the zero sequence row $[\text{C}_0]$, $[\text{C}]$ can be completed by introducing a second zero-sequence component $i_0^-$ through an additional row $[\text{C}_0^-]$.

To establish whether a set of space vectors can be freely controlled it is sufficient to compute the rank of the matrix built by considering the corresponding rows $[\text{C}_h]$ (defined as per (8)) and the zero-sequence row $[\text{C}_0]$: indeed, when some rows are

linearly dependent on some others, there are certain algebraic constraints between the corresponding space vector components. Therefore, to get full control of both $\mathbf{i}_1$ and $\mathbf{i}_3$, which will be exploited in Section III by the proposed strategy, the Clarke transformation matrix should be built as:

$$[C]=\begin{bmatrix} [C_1] \\ [C_{-1}] \\ \vdots \\ ([C_0^-]) \\ [C_0] \end{bmatrix} \quad \text{with } [i_{VSD}]=[i_{x1},i_{y1},i_{x3},i_{y3},\dots]^T \tag{9}$$

In (9), the higher order rows should be chosen, wherever possible, to take advantage of the space vectors associated with the highest torque gain factors $\kappa_h$ (usually the ones which drive the lowest odd-order spatial harmonics). Once the set $[i_{VSD}]$ has been chosen, its relationship with any other $h$-th space vector components $\{i_{xh},i_{yh}\}$ is found to be:

$$[i_{xh}\ i_{yh}]^T=[C_h]\cdot[i_{ph}]=[C_h]\cdot[T]\cdot[i_{VSD}] \tag{10}$$

In the case of a symmetrical machine with an odd number of phases the magnetic axes are $\alpha_k=(k-1)\cdot(2\pi/n)$ and it can be verified that, by choosing the space vectors linked to the smallest $(n-1)/2$ odd-order spatial harmonics, the resulting Clarke matrix [C] is guaranteed to be unitary (i.e. invertible and such that $[T]=[C]^{-1}=[C]^T$). This property is however not guaranteed in a generic configuration, as exemplified for the asymmetrical nine-phase PMSM in [22].

## D. Choice of the Rotational Transformation

Once the Clarke's transformation matrix [C] has been built to control a given set of space vectors, the VSD current set $[i_{VSD}]$ can be linked to the corresponding synchronous set $[i_{dq}]$ through a rotational transformation:

$$[i_{dq}]=[D](\theta)\cdot[i_{VSD}] \quad \Leftrightarrow \quad [i_{VSD}]=[D]^{-1}(\theta)\cdot[i_{dq}] \tag{11}$$

Given (5), the rotational matrix $[D](\theta)$ can be obtained by properly combining a set of submatrices $[D_h](\theta)$ built as:

$$\begin{bmatrix} i_{dh} \\ i_{qh} \end{bmatrix}=[D_h](\theta)\cdot\begin{bmatrix} i_{xh} \\ i_{yh} \end{bmatrix}=\begin{bmatrix} \cos(h\theta+\varphi_h) & \sin(h\theta+\varphi_h) \\ -\sin(h\theta+\varphi_h) & \cos(h\theta+\varphi_h) \end{bmatrix}\cdot\begin{bmatrix} i_{xh} \\ i_{yh} \end{bmatrix} \tag{12}$$

The rotational matrix associated to (9), which selects the $\mathbf{i}_1^{\langle dq\rangle}$ and $\mathbf{i}_3^{\langle dq\rangle}$ components, takes the block-diagonal form:

$$[D](\theta)=\begin{bmatrix} [D_1](\theta) & [0_{2\times2}] & \cdots & [0_{2\times1}] \\ [0_{-1}] & [D_{-1}](\theta) & \cdots & [0_{-1}] \\ \vdots & \vdots & \ddots & \vdots \\ ([0_{1\times2}]) & ([0_{1\times2}]) & \cdots & (0) \\ [0_{1\times2}] & [0_{1\times2}] & \cdots & 1 \end{bmatrix} \tag{13}$$

with $[i_{dq}]=[i_{d1},i_{q1},i_{d3},i_{q3},\dots,i_0^-,i_0]^T$. Generally speaking, once the set $[i_{VSD}]$ contains both the real and imaginary part of each chosen space vector $\mathbf{i}_h$, the rotational matrix, built by combining the submatrices defined as per (12), can be verified to be unitary (i.e. $[D]^{-1}(\theta)=[D]^T(\theta)$).

## E. Power Loss Expression

Considering (7) and (11) and neglecting all losses except for those in the stator windings, the instantaneous power losses can be expressed in terms of the transformed current set $[i_{dq}]$:

$$p=R\cdot\sum_{k=1}^{n}i_k^2=R\cdot[i_{ph}]^T\cdot[i_{ph}]=R\cdot[i_{dq}]^T\cdot[G](\theta)\cdot[i_{dq}] \tag{14}$$

with $[G](\theta)=[D](\theta)\cdot[T]^T\cdot[T]\cdot[D]^T(\theta)$. Then, the average power losses can be found by averaging $p$ along a full rotor cycle. For a constant synchronous current set $[i_{dq}]$ each component is independent of $\theta$ and the result is expressed as:

$$P=(1/2\pi)\cdot\int_0^{2\pi}p(\theta)\mathrm{d}\theta=R\cdot[i_{dq}]^T\cdot[H]\cdot[i_{dq}] \tag{15}$$

where $[H]=(1/2\pi)\cdot\int_0^{2\pi}[G](\theta)\mathrm{d}\theta$.

It can be verified that all the non-diagonal terms of $[G](\theta)$ are trigonometric functions with a zero average value over a full cycle of $\theta$ and that the diagonal terms corresponding to the same $h$-th space vector have an equal average value $H_h>0$ over a full electric rotation angle. Therefore, the matrix [H] related to (9) and (13) is positive definite and assumes the diagonal form:

$$[H]=\begin{bmatrix} H_1 & 0 & 0 & 0 & \cdots & 0 \\ 0 & H_1 & 0 & 0 & \cdots & 0 \\ 0 & 0 & H_3 & 0 & \cdots & 0 \\ 0 & 0 & 0 & H_3 & \cdots & 0 \\ \vdots & \vdots & \vdots & \vdots & \vdots & \vdots \\ (0) & (0) & (0) & (0) & \cdots & (0) \\ 0 & 0 & 0 & 0 & \cdots & H_0 \end{bmatrix} \tag{16}$$

To summarize, once [C] has been chosen, both [T] and $[D](\theta)$ are univocally identified. Consequently, it is possible to compute the instantaneous loss weighting matrix $[G](\theta)$, from which, by operating an element-by-element average process, the matrix [H] is derived. For a symmetrical machine, since [C] is unitary, it follows that $[G](\theta)=[H]=[I_{n\times n}]$.

## F. Transformed Electrical Equations

Once the transformation matrices [C] and $[D](\theta)$ have been chosen, they can be applied to all the variables in (2). By using the VSD transformation (7) the model is modified as:

$$\begin{cases} [u_{VSD}]+v_{ON}\cdot[c]=[v_{VSD}]=R\cdot[i_{VSD}]+[L_{VSD}]\cdot\dfrac{\mathrm{d}}{\mathrm{d}t}[i_{VSD}]+[e_{VSD}] \\ i_0=[0\ 0\ \cdots\ 1]\cdot[i_{VSD}]=0 \end{cases} \tag{17}$$

with $[c]=[C]\cdot[1_{n\times1}]$ and $[L_{VSD}]=[C]\cdot[L]\cdot[T]$.

For a machine with a symmetrical winding configuration and an odd number of phases, the inductance matrix $[L]$ has a circular structure (i.e. $L_{j,k}=L_{j+1,k+1}$). If, again, the space vectors linked to the smallest $(n-1)/2$ odd-order spatial harmonics are selected, the rows of the matrix [C] (and, given the unitary property, also the columns of $[T]=[C]^T$) are the eigenvectors of the matrix $[L]$. As a result, the matrix $[L_{VSD}]=[C]\cdot[L]\cdot[C]^T$ is diagonal and effectively performs the decoupling of the different components of the $[i_{VSD}]$ set. On the contrary, for a generic configuration this property is not guaranteed (as shown in [22] for a nine-phase asymmetrical machine).

By applying the rotational transformation (11) to the system (17), the model becomes:

$$\begin{cases} [u_{dq}]+v_{ON}\cdot[g](\theta)=[v_{dq}]=R\cdot[i_{dq}]+\dots \\ \quad\dots\quad (\theta)\cdot\dfrac{\mathrm{d}}{\mathrm{d}t}[i_{dq}]+\omega\cdot[L_{dq2}](\theta)\cdot[i_{dq}]+[e_{dq}] \\ i_0=[0\ 0\ \cdots\ 1]\cdot[i_{dq}]=0 \end{cases} \tag{18}$$

with $[g](\theta)=[D](\theta)\cdot[c]$, $[L_{dq1}](\theta)=[D](\theta)\cdot[L_{VSD}]\cdot[D]^T(\theta)$ and $[L_{dq2}](\theta)=[D](\theta)\cdot[L_{VSD}]\cdot(\partial[D]^T(\theta)/\partial\theta)$. Again, the different components of $[i_{dq}]$ can exhibit a coupling effect both through the transformed inductance matrices $[L_{dq1}](\theta)$, $[L_{dq2}](\theta)$ and through the term $v_{ON}\cdot[g](\theta)$. Indeed, the neutral point potential shift $v_{ON}$ generally depends not only on the voltage sets $[e_{dq}]$ and $[u_{dq}]$, but also on the current set $[i_{dq}]$: the formal relationship can be found by imposing the constraint $i_0=0$ and the subsequent condition $\mathrm{d}i_0/\mathrm{d}t=0$ in the zero-sequence subspace equation of (18). Once substituted back in the other subspace equations, it allows to explicitly highlight the additional mutual coupling between the current components.

## III. Optimal Third Harmonic Injection Strategy

Standard field oriented control (FOC) algorithms, developed for isotropic PMSMs, only control the $i_{q1}$ current component of the $[i_{dq}]$ set, while keeping all the other terms to zero. Consequently, the reference current $i_{q1}^* = T_{em}^*/\kappa_1$ is proportional to the desired torque $T_{em}^*$ and the overall average power losses are $P_{FUND} = R\,H_1\,(T_{em}^*/\kappa_1)^2$. For a constant rotor speed, the resulting reference phase currents are sinusoidal.

However, in the presence of significant higher order spatial harmonics in the PMs' induced flux density, it is possible to exploit the quadrature component of some higher order current space vectors as available degrees of freedom for the torque development. Then, given the higher number of degrees of freedom, it is possible to formulate an optimal strategy to choose the current references while keeping the supplied torque to the desired reference $T_{em}^*$.

The proposed strategy aims to minimize the average stator power losses for a given torque by using a constant synchronous current set $[i_{dq}^*]$. Under the reasonable hypothesis that all the even-order spatial harmonics are absent and that the odd-order ones with index $h \geq n$ are negligible, the torque expression (6) is a linear combination of the synchronous current set component contributions, which can be synthetically formulated by introducing the $n\times 1$ torque gain vector as:

$$[\kappa] = P_p\sqrt{n/2}\cdot[0\ \lambda_{M1}\ 0\ 3\lambda_{M3}\ \cdots \tag{19}$$

resulting in $T_{em}=[\kappa]^T\cdot[i_{dq}]$. Since $[\kappa]$ is independent from $\theta$, it allows for an optimization with a constant $[i_{dq}^*]$ vector.

Then, the simplest enhancement can be obtained through the control of the $i_{q3}$ current component. In steady state conditions at a constant speed, due to the $3\theta$ rotation in the $[D](\theta)$ matrix, the application of a constant $i_{q3}$ corresponds to a third harmonic current injection into each phase current. All the other components of $[i_{dq}]$ can be set to zero not to interfere either with the torque development or with the power dissipation.

Then, the function to minimize is $P = R\cdot(H_1 i_{q1}^2 + H_3 i_{q3}^2)$, under the equality constraint represented by the reference torque development $T_{em}^* = \kappa_1 i_{q1} + \kappa_3 i_{q3}$.

The average power losses can be expressed as a function of the third harmonic injection ratio $k = i_{q3}/\,i_{q1}$ as:

$$P(k) = R\cdot(T_{em}^*)^2\cdot(H_1 + H_3 k^2)/(\kappa_1 + \kappa_3 k)^2 \tag{20}$$

The function (20) is convex with respect to $k$ and its minimum value can be found by forcing to zero its derivative $\partial P/\partial k$. The optimal injection ratio is:

$$k_{opt} = (\kappa_3/\kappa_1)/(H_3/H_1) \tag{21}$$

and the corresponding optimal currents are:

$$i_{q1}^* = \frac{H_3\,\kappa_1}{H_1\,\kappa_3^2 + H_3\,\kappa_1^2}T_{em}^*;\quad i_{q3}^* = \frac{H_1\,\kappa_3}{H_1\,\kappa_3^2 + H_3\,\kappa_1^2}T_{em}^* \tag{22}$$

The average power losses with the optimal injection ratio are:

$$P_{opt} = R\cdot(T_{em}^*)^2\cdot(H_1H_3)/(\kappa_3^2H_1 + \kappa_1^2H_3) \tag{23}$$

and can be compared to the ones generated by a traditional strategy which only exploits $i_{q1}$, leading to a ratio of:

$$\eta_{opt} = P_{opt}/P_{FUND} = (\kappa_1^2H_3)/(\kappa_3^2H_1 + \kappa_1^2H_3) \tag{24}$$

From the set $[i_{dq}^*]$, whose $i_{q1}^*$ and $i_{q3}^*$ components are chosen via (22), the optimal phase current set $[i_{ph}^*]$ can be found by applying the inverse transformations (7) and (11).

## IV. Application Examples

To highlight the generality of the approach, the strategy is discussed further on in detail for a selected set of phase numbers, for machines with asymmetrical winding topology.

### A. Six-Phase Asymmetrical Machine

The machine windings can be grouped in two symmetrical three-phase sets $\{a_1,b_1,c_1\}$ and $\{a_2,b_2,c_2\}$ whose magnetic axes are mutually shifted by 30° electrically. The corresponding electrical angle set is $[\alpha] = [0°\ 120°\ 240°\ |\ 30°\ 150°\ 270°]$. By examining via (8) the rows $[C_3]$ related to the third harmonic space vector $\mathbf{i}_3$ one gets:

$$[C_3] = \sqrt{1/3}\cdot\begin{bmatrix}1 & 1 & 1 & 0 & 0 & 0\\ 0 & 0 & 0 & 1 & 1 & 1\end{bmatrix} \tag{25}$$

This set of rows is linearly dependent on the zero-sequence row $[C_0] = [1\ 1\ 1\ 1\ 1\ 1]/\sqrt{6}$. Since $i_0$ is constrained to zero by the single isolated neutral point configuration, $i_{x3}$ and $i_{y3}$ cannot be independently controlled at the same time. As a result, it is impossible to generate a rotating space vector $\mathbf{i}_3$ and the third harmonic current injection cannot be exploited for the torque development unless there is an additional conductor allowing $i_0 \neq 0$ (as in [19-21] with the seventh inverter leg or with a direct connection of the neutral point $N$ to the dc link midpoint $O$).

### B. Nine-Phase Asymmetrical Machine

This configuration has been examined by the authors in [22]. The machine windings can be grouped in three symmetrical three-phase sets $\{a_1,b_1,c_1\}$, $\{a_2,b_2,c_2\}$ and $\{a_3,b_3,c_3\}$ whose magnetic axes are mutually shifted by 20° electrically; the corresponding electrical angle set is $[\alpha] = [0°\ 120°\ 240°\ |\ 20°\ 140°\ 260°\ |\ 40°\ 160°\ 280°]$.

It can be verified that the Clarke's matrix [C] chosen to control the space vectors $\mathbf{i}_1$, $\mathbf{i}_3$, $\mathbf{i}_5$ and $\mathbf{i}_7$ is a full rank matrix. The evaluation of the [H] matrix has been performed analytically, resulting in $H_1 = 1$; $H_3 = 5$; $H_5 = 1$; $H_7 = 1$ and $H_0 = 9$.

The strategy has been particularized with respect to the real prototype described in [22-23], whose PM flux parameters are summarized in Table I; for simplicity, the contribution of the harmonics with order $h > 7$ has been neglected.

TABLE I PM Induced Flux Harmonic Parameters

| Harmonic Order $h$ | 1 | 3 | 5 | 7 |
|---|---|---|---|---|
| $\lambda_{Mh}$ [mWb] | 385 | 119 | 38 | 7 |
| $\varphi_h$ [deg] | 0° | ≅ 180° | ≅ 0° | ≅ 165° |

Fig. 2 shows the normalized power losses obtained when both $i_{q1}$ and $i_{q3}$ are exploited for the torque development. Consistently with (21) and (24), the minimum power ratio

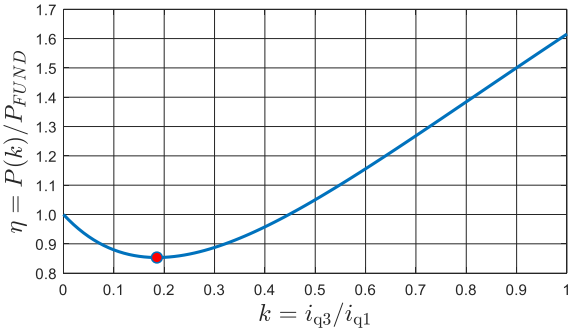


Fig. 2. Average losses in the asymmetrical nine-phase machine case..

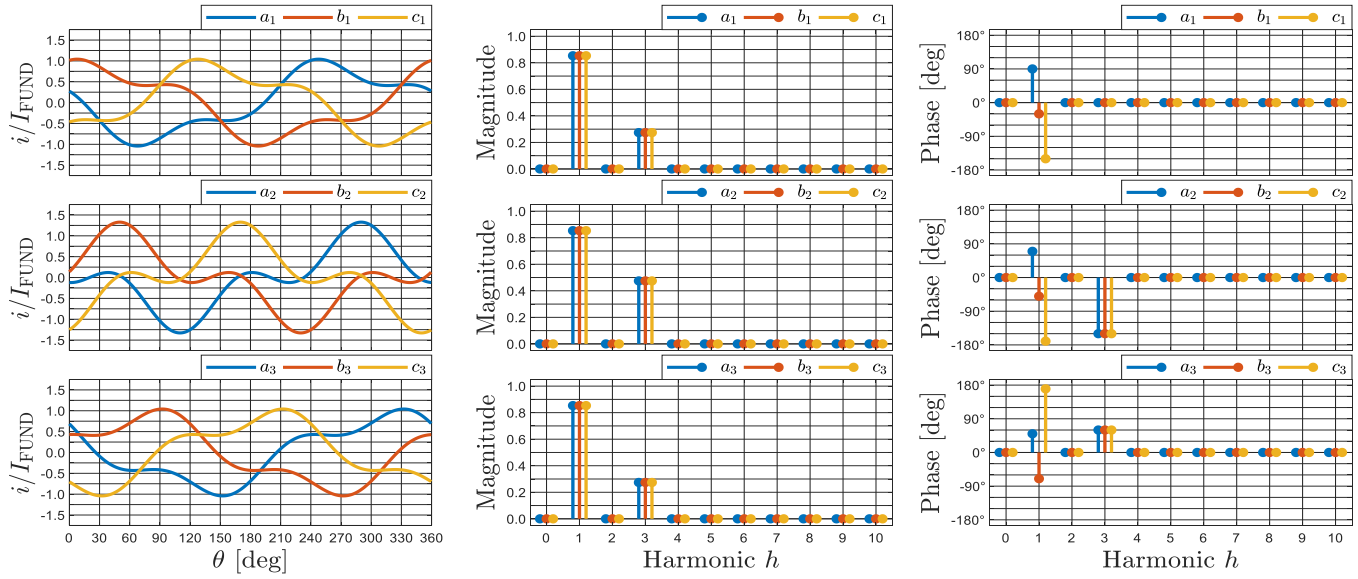


Fig. 3. Optimal phase current waveforms and harmonic spectra for the asymmetrical nine-phase machine.

$\eta \cong 0.85$ (highlighted by the red dot in Fig. 2) is obtained for $k \cong 0.19$ and corresponds to a 15% power loss reduction.

The optimal phase current waveforms and their spectra are depicted in Fig. 3, normalized by $I_{FUND} = (2/9)\cdot T^*_{em}/\lambda_{M1}$, which represents the peak phase current needed to supply the same torque by only exploiting the fundamental harmonic $i_{q1}$. In accordance with the analytical results, only the 1st and 3rd harmonics are present in the Fourier decomposition. The waveforms of each three-phase $\{a,b,c\}$ set are identical and just mutually shifted by 120°. Nevertheless, it can be immediately noticed that the different sets behave differently from each other. This results in the unequal injection of the third harmonic components which, in order to satisfy the condition $i_0 = 0$, are not evenly distributed among the different phase sets. In particular, the magnitude in the first and the third set is equal, while the magnitude in the second set is $\sqrt{3}$ times higher. This unequal distribution of the currents leads to an unequal distribution of the power losses (31.3% for the 1st and 3rd sets, 37.4% for the 2nd set). Finally, it can also be noted that, despite the reduction of the root mean square (RMS) with respect to the sole exploitation of $i_{q1}$, the normalized peak current values are higher than 1, and the $\{a_2,b_2,c_2\}$ is the most affected set.

## C. Twelve-Phase Asymmetrical Machine

In this case the machine windings can be grouped in four symmetrical three-phase sets $\{a_p,b_p,c_p\}$ (with $p = 1,\ldots,4$), whose magnetic axes are mutually shifted by 15°. The machine parameters are still assumed to be the same as those in Table I.

From the analysis of the angle set it can be verified that the rectangular matrix built with $[C_1]$, $[C_3]$ and $[C_0]$ has a rank 5, meaning that it is possible to independently control both $\mathbf{i}_1$ and $\mathbf{i}_3$ and, therefore, exploit the third harmonic contribution for the torque development. However, the rows $[C_9]$ are linearly dependent on the rows $[C_1]$, $[C_3]$ and $[C_0]$, meaning that the control of $\mathbf{i}_1$ and $\mathbf{i}_3$ makes it impossible to simultaneously control also $\mathbf{i}_9$. As a result, for the considered case study, the matrix [C] has been built by choosing the rows related to the space vectors $\mathbf{i}_1$, $\mathbf{i}_3$, $\mathbf{i}_5$, $\mathbf{i}_7$, and $\mathbf{i}_{11}$, while the second zero sequence component $i_0^-$ has been arbitrarily defined through the row $[C_0^-] = \sqrt{1/6}\cdot[1\ 1\ 1\ {-1}\ {-1}\ {-1}\ 1\ 1\ 1\ {-1}\ {-1}\ {-1}]$. The analytical evaluation of the matrix [H] results in $H_1 = 1$; $H_3 = 4$; $H_5 = 1$; $H_7 = 1$; $H_{11} = 1$; $H_{0^-} = 2 - \sqrt{2}$ and $H_0 = 2\cdot(2 + \sqrt{2})$.

Fig. 4 shows the normalized power losses obtained by exploiting $i_{q1}$ and $i_{q3}$ with a varying injection ratio. Again, in accordance with (21) and (24), the minimum value is obtained for $k \cong 0.23$ and it leads to the power ratio $\eta \cong 0.82$, corresponding to power loss reduction of about 18%.

The optimal phase current waveforms and their spectra are depicted in Fig. 5, normalized by $I_{FUND} = (2/12)\cdot T^*_{em}/\lambda_{M1}$. As in the previous case, only the 1st and 3rd harmonics are present in the current spectra. Again, the waveforms of each three-phase $\{a,b,c\}$ set are identical and just mutually shifted by 120°, while the different sets behave differently from each other. However, in contrast to the nine-phase machine, in this case the magnitude of the third harmonic component is equal in all the windings, meaning that the overall power losses are equally distributed among all the phases. In particular, the third harmonic current components have the same phase in each set, and the pairs $\{a_1,b_1,c_1\}$-$\{a_3,b_3,c_3\}$ and $\{a_2,b_2,c_2\}$-$\{a_3,b_4,c_4\}$ show an opposite sign. This is a direct consequence of the arbitrary definition of $i_0^-$. Indeed, the control condition $i_0^- = 0$ (resulting from the choice of $[C_0^-]$ and from the optimization with a constant $[i_{dq}]$ set), together with the winding constraint $i_0 = 0$, corresponds to:

$$i_{a_1}+i_{b_1}+i_{c_1}+i_{a_3}+i_{b_3}+i_{c_3}=0\ ;\quad i_{a_2}+i_{b_2}+i_{c_2}+i_{a_4}+i_{b_4}+i_{c_4}=0 \qquad (26)$$

which reflect the constraints imposed to a system built from two isolated asymmetrical six-phase winding sets shifted by 15°.

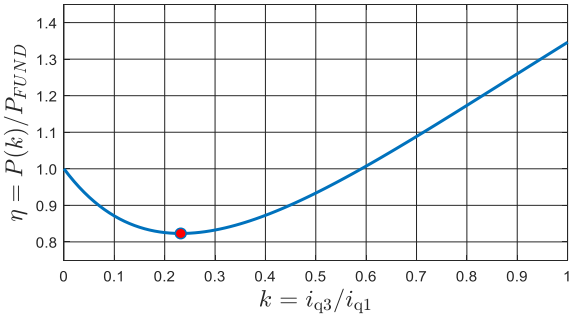


Fig. 4. Average loss in the asymmetrical twelve-phase machine case .

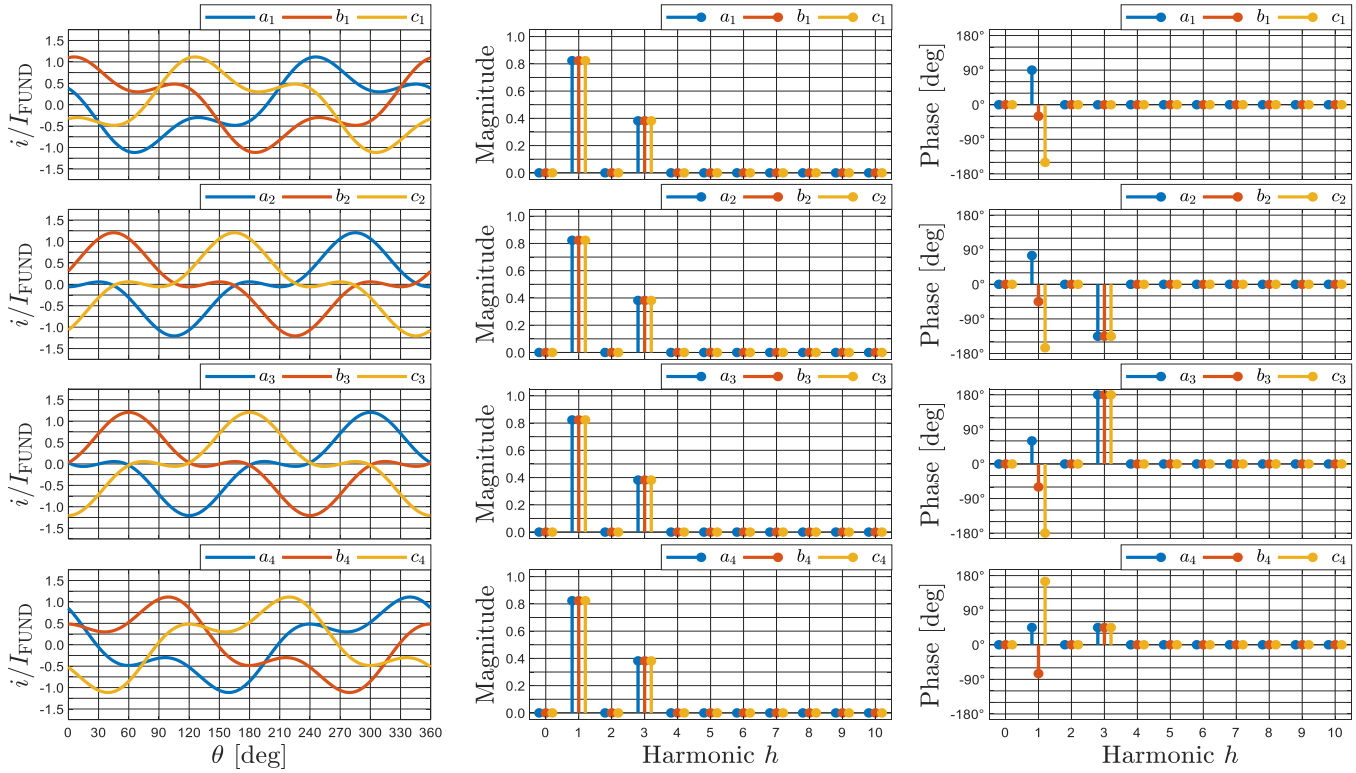


Fig. 5. Optimal phase current waveforms and harmonic spectra for an asymmetrical twelve-phase machine.

In this context, the capability of enhancing the torque generation by controlling $\mathbf{i}_3$ might lead to an apparent contradiction since, as previously stated, it is impossible to exploit the third harmonic injection in an asymmetrical six phase machine. However, for the considered twelve-phase machine, $\mathbf{i}_3$ results from the superposition of the third harmonic space vectors $\mathbf{i}_3^{[A]}$ and $\mathbf{i}_3^{[B]}$ driven by the currents of the two six-phase windings sets. By denoting as $I_3$ the magnitude of the optimal 3rd harmonic component in the phase domain it can be verified that these space vectors can be expressed as $\mathbf{i}_3^{[A]} = 3\sqrt{2}\,M_3 I_3 \cos(3\theta)\mathrm{e}^{-\mathrm{j}\pi/4}$ and $\mathbf{i}_3^{[B]} = 3\sqrt{2}\,M_3 I_3 \cos(3\theta - 3\pi/4)$: they generate two pulsating fields in the machine's air-gap and the resulting twelve-phase space vector is equal to $\mathbf{i}_3 = \mathbf{i}_3^{[A]} + \mathbf{i}_3^{[B]} = 3M_3 I_3 \mathrm{e}^{\mathrm{j}(3\theta - \pi/2)}$, which yields a rotating field at a $3\omega$ angular frequency and justifies the unexpected property. From a different perspective, it is possible to observe in Fig. 6 the torques (calculated analytically) generated by applying the optimal reference currents to the two six-phase winding sets: the two contributions present an average value of $T^*_{em}/2$ and a superimposed oscillation varying with $6\theta$. A single six-phase contribution would not be able to guarantee a constant output torque, whereas their sum cancels out the sinusoidal oscillation.

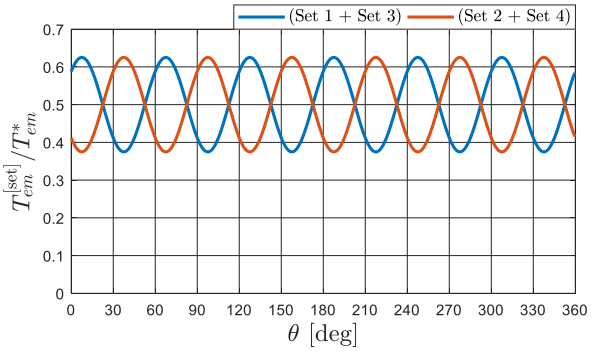


Fig. 6. Torques produced by the two six-phase windings sets.

## D. Fifteen-Phase Asymmetrical Machine

The machine windings are here grouped into five symmetrical three-phase sets $\{a_p,b_p,c_p\}$ (with $p = 1,\ldots,5$), whose magnetic axes are mutually shifted by 12°. Once again, the machine parameters are assumed to be the ones of Table I.

From the analysis of the corresponding Clarke's matrix [C], it can be verified that all the odd-order space vectors up to $\mathbf{i}_{13}$ can be independently controlled at the same time. The evaluation of the matrix [H] results in $H_1 = 1$; $H_3 = 7 + 2\sqrt{5}$; $H_5 = 1$; $H_7 = 1$; $H_9 = 7 - 2\sqrt{5}$; $H_{11} = 1$; $H_{13} = 1$ and $H_0 = 25$.

Fig. 7 shows the normalized power losses obtained with the third harmonic injection. The minimum value is obtained for $k \cong 0.08$ and it leads to the power ratio $\eta \cong 0.93$, corresponding to power loss reduction of about 7%; the optimal phase current waveforms and their spectra are depicted in Fig. 8, normalized by $I_{FUND} = (2/15)\cdot T^*_{em}/\lambda_{M1}$.

As in the previous cases, the waveforms of each three-phase $\{a,b,c\}$ set are identical and just mutually shifted by 120°, while

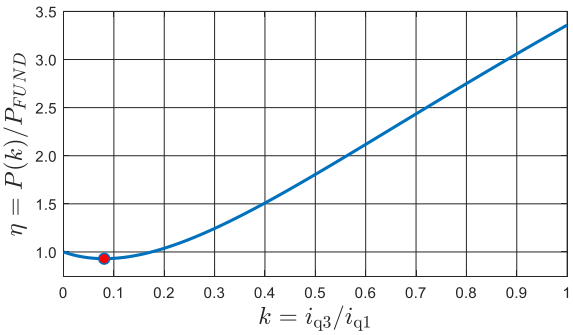


Fig. 7. Average loss in the asymmetrical fifteen-phase machine case.

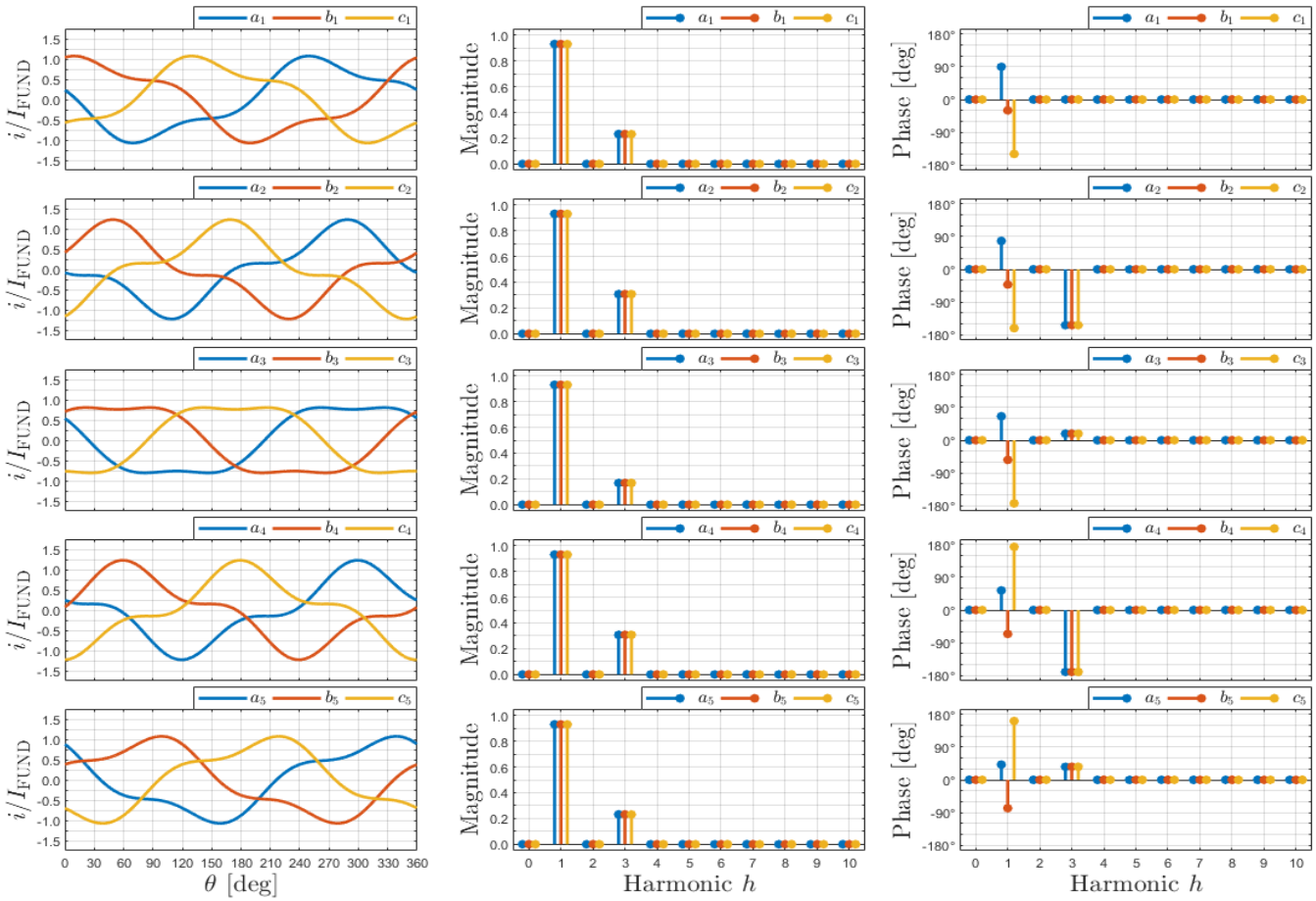


Fig. 8. Optimal phase current waveforms and harmonic spectra for the asymmetrical fifteen-phase machine.

the different sets behave differently. Similarly to the nine-phase example, in order for the condition $i_0 = 0$ to be satisfied, the third harmonic component is not equally shared by all the windings. Once again, this leads to an unequal distribution of the power losses among the different winding sets. It can be verified from the harmonic spectra that the 1st and 5th sets have the same magnitude for all the harmonics and, therefore, the same RMS. Each of them is responsible for about 19.76% of the total losses. Analogously, the 2nd and 4th sets behave in the same way and are responsible for about the 20.64% of the total losses, each. Finally, the remaining 19.20% of the losses are dissipated by the 3rd three-phase set.

### E. Five-Phase Asymmetrical Machine

This case study focuses on an asymmetrical five-phase machine, obtained from an original symmetrical seven-phase machine after a post-fault reconfiguration in which two adjacent phase windings (i.e. mutually shifted by 360°/7) have been physically disconnected. The resulting phases (further on referred to as $\{a,b,c,d,e\}$) can be identified through the magnetic axis angles set $[\alpha] = [0\ 1\ 2\ 3\ 4]\cdot(360°/7)$. It is assumed that only the 1st and the 3rd spatial harmonics are present in the permanent magnet flux ($h < n$ assumption) for simplicity and that the PM's induced fluxes have the same values as in the previous examples (that is, $\lambda_{M1} = 385$ mWb, $\varphi_1 = 0°$, $\lambda_{M3} = 119$ mWb, $\varphi_3 \cong 180°$).

The Clarke's transformation matrix, built using $[C_1]$, $[C_3]$ and $[C_0]$, is full-ranked and the evaluation of the weighting matrix [H] results in $H_1 \cong 1.570$, $H_3 \cong 1.315$ and $H_0 \cong 1.633$.

Fig. 9 shows the normalized power losses for a varying injection ratio: in this case, the optimal injection ratio is obtained for $k \cong 1.11$ (i.e. $i_{q3} > i_{q1}$), resulting in $\eta \cong 0.49$ and thus leading to a power loss reduction of more than 50%.

Fig. 10 shows the phase current waveforms and their corresponding harmonic spectra, first when the machine is controlled by only exploiting $i_{q1}$ (top plots) and then when $i_{q3}$ is simultaneously controlled with the optimal injection ratio (bottom graphs). All the currents have been normalized by $I_{FUND} = (2/7)\cdot T^*_{em}/\lambda_{M1}$, which is the peak value of the phase currents obtained when the original (i.e. symmetrical seven-phase) machine is driven by only the fundamental current components.

As can be seen, in contrast to the previous examples, in this case the phase current waveforms are mutually different even when only the fundamental component is controlled. In both operating conditions the magnitudes of the harmonic components of phase *a* are equal to the ones of phase *e*, while the magnitudes of the harmonic components of phase *b* are

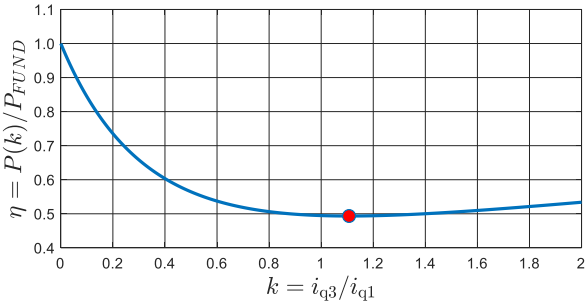


Fig. 9. Average loss in the asymmetrical five-phase machine case study.

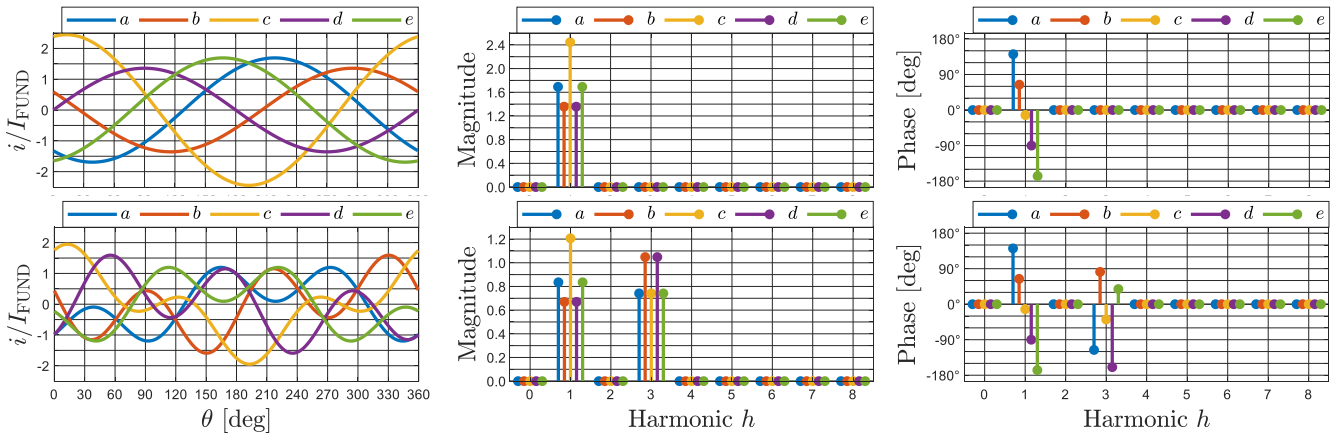


Fig. 10. Phase current waveforms and harmonic spectra for the asymmetrical five-phase machine (Top: fundamental only. Bottom: optimal third harmonic injection).

equal to the ones of phase *d*. They differ from those in phase *c*.

When only the 1st harmonic component is exploited, phases *a* and *e* are responsible for 18.61% of the overall losses each, phase *b* and *d* are responsible for 11.97% each, while phase *c* is responsible for the remaining 38.85%. By injecting the optimal third harmonic current component, the power losses in phase *a* and *e* reduce and are 16.42% of the total, the losses in phase *b* and *d* increase and become 20.38% of the total, while the power dissipated in phase *c* is lowered to 26.41% of the overall losses. It can be concluded that, for the considered example, the harmonic injection is able to not only drastically improve the machine's overall energetic performances, but it is also responsible for a better redistribution of the power losses, if compared to the solely fundamental excitation. Moreover, the peak current of phase *c* (which, in both scenarios, is the highest one) is reduced by around 20% thanks to the reduction of the fundamental component allowed by the injection of the additional third harmonics.

## V. Numerical and Experimental Results

The proposed approach has been numerically and experimentally validated with respect to the asymmetrical nine-phase machine described in [22-23]. From the analysis of the electrical equations in the synchronous domain (obtained through (18)) it can be verified that the 1st, 5th and 7th space vector subspaces are decoupled, resulting in [22]:

$$\begin{cases} u_{dh} = v_{dh} = Ri_{dh} + L_h \dfrac{\mathrm{d}i_{dh}}{\mathrm{d}t} - h\omega L_h i_{qh} \\ u_{qh} = v_{qh} = Ri_{qh} + L_h \dfrac{\mathrm{d}i_{qh}}{\mathrm{d}t} + h\omega L_h i_{dh} + e_{qh} \end{cases} \tag{27}$$

with $h = 1,5,7$ and $e_{qh} = \sqrt{9/2}h\omega\lambda_{Mh}$. The 3rd space vector subspace is instead coupled with $v_{ON}$ by [g]($\theta$) [22]:

$$\begin{cases} u_{d3} + 2\sqrt{2}\cos(3\theta+\varphi_3-\pi/3)\cdot v_{ON} = v_{d3} = Ri_{d3} + L_3 \dfrac{\mathrm{d}i_{d3}}{\mathrm{d}t} - 3\omega L_3 i_{q3} \\ u_{q3} + 2\sqrt{2}\cos(3\theta+\varphi_3+\pi/6)\cdot v_{ON} = v_{q3} = Ri_{q3} + L_3 \dfrac{\mathrm{d}i_{q3}}{\mathrm{d}t} + 3\omega L_3 i_{d3} + e_{q3} \end{cases} \tag{28}$$

with $e_{q3}=9/\sqrt{2}\omega\lambda_{M3}$. It should also be noted that, given the asymmetrical winding configuration, $v_{ON}$ is itself dependent on the currents ($i_{d3}$,$i_{q3}$). Indeed, by imposing the conditions $i_0 = 0$ and $\mathrm{d}i_0/\mathrm{d}t = 0$ in the zero-sequence equation of the model (18), the following functional relationship is obtained:

$$\begin{cases} v_{ON} = \dfrac{L_{m3}}{9}\left[\left(2\sqrt{2}\sin(3\theta+\varphi_3+\pi/6)\right)\left(\dfrac{\mathrm{d}i_{d3}}{\mathrm{d}t} - 3\omega i_{q3}\right) + \ldots \right. \\ \left. \ldots + \left(2\sqrt{2}\cos(3\theta+\varphi_3+\pi/6)\right)\left(\dfrac{\mathrm{d}i_{q3}}{\mathrm{d}t} + 3\omega i_{d3}\right)\right] + \dfrac{e_0 - u_0}{3} \end{cases} \tag{29}$$

with $L_{m3}=L_3 - L_l$ and $e_0=-6\omega\lambda_{M3}\sin(3\theta+\varphi_3-\pi/3)$. The additional coupling terms arising among the ($i_{d3}$,$i_{q3}$) components, which can be identified by substituting (29) in (28), need to be properly compensated in the current control. It is important to highlight that the supplying inverter's common mode voltage influences both $u_0$ and ($u_{d3}$,$u_{q3}$) at the same time, such that their simultaneous changes cancel out and do not affect the ($i_{d3}$,$i_{q3}$) current dynamics. Therefore, the compensation of $e_0$ can be achieved either by acting on $u_0$ or by acting on both $u_{d3}$ and $u_{q3}$.

The machine under analysis has one pole pair, its flux parameters correspond to the ones reported in Table I, while its electrical parameters are reported in Table II.

TABLE II NINE-PHASE MACHINE ELECTRICAL PARAMETERS

| | | |
|---|---|---|
| $R = 31.3\ \Omega$ | $L_1 = 147$ mH | $L_5 = 88$ mH |
| $L_l = 84$ mH | $L_3 = 92$ mH | $L_7 = 87$ mH |

### A. Simulation Results

The numerical results have been obtained in the Matlab/Simulink environment. The implemented control algorithm is schematically represented in Fig. 11.

The 'Injection Strategy' block finds the references $i^*_{q1}$ and $i^*_{q3}$ able to develop the desired electromagnetic torque $T^*_{em}$ for a given injection ratio $k = i^*_{q3}/i^*_{q1}$; obviously, when $k = k_{opt}$ the block implements the developed optimal injection strategy and selects the references according to (22). All the other components of the reference set $[i^*_{dq}]$ are zero.

Since the reference current set $[i^*_{dq}]$ is constant, a proportional-integral (PI) controller has been used to drive all the components of the synchronous current set $[i_{dq}]$ (with the only exception of $i_0 = 0$ which, obviously, cannot be controlled due to the hardware constraint). While the compensation terms in the 1st, 5th and 7th space vectors' subspaces are obtained by the standard FOC approach, the 3rd space vector subspace needs an additional compensation term to neutralize the effects of $v_{ON}$.

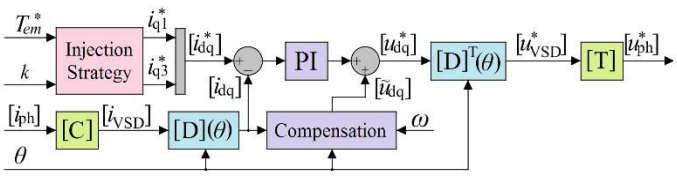


Fig. 11. Control scheme.

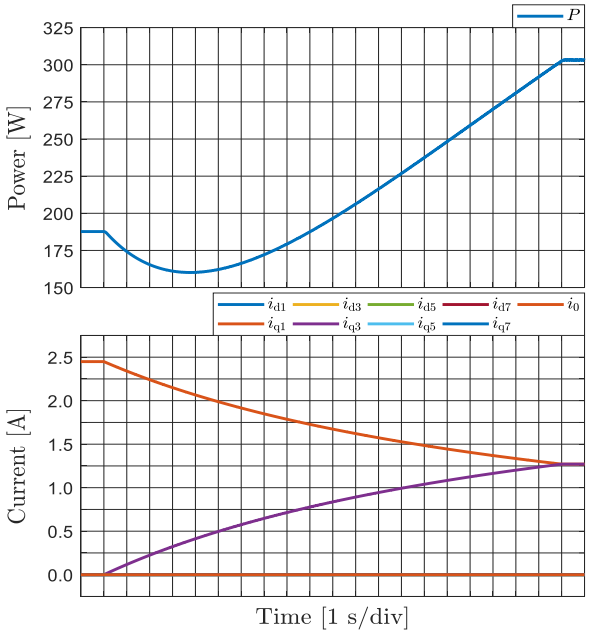


Fig. 12. Simulation results for the asymmetrical nine-phase case.

Based on the model equations (27)-(29), the 'Compensation' block represented in Fig. 11 computes the voltage set $[\tilde{u}_{dq}]$ through the relations:

$$\left.\begin{aligned} \tilde{i} &= r_h i_{qh} \\ \tilde{i} &= r_h i_{dh} + e_{qh} \end{aligned}\right\} \text{ with } h = 1,5,7$$
$$\tilde{i} = r_3 i_{q3} - 2\sqrt{2}\cos(3\theta + \varphi_3 - \pi/3)\cdot\tilde{} \qquad (30)$$
$$\tilde{i} = r_3 i_{d3} - 2\sqrt{2}\cos(3\theta + \varphi_3 + \pi/6)\cdot\tilde{}$$
$$\tilde{i} = 6\omega\lambda_{M3}\sin(3\theta + \varphi_3 - \pi/3)$$

with $\tilde{v}_{ON}=(2\sqrt{2}\omega L_{m3}/3)[i_{d3}\cos(3\theta+\varphi_3+\pi/6)-i_{q3}\sin(3\theta+\varphi_3+\pi/6)]$. The resulting vector is added to the output of the current PI controllers and it represents the synchronous voltage set $[u^*_{dq}]$, which is finally transformed into the corresponding inverter's reference voltage set $[u^*_{ph}]$ by applying the inverse transformations (7) and (11).

The control algorithm has been implemented in discrete time with a 10 kHz sampling frequency. The supplying inverter has been simulated through an average model to filter out the high frequency harmonics introduced by the Pulse Width Modulation (PWM) technique.

Fig. 12 shows the simulation results obtained by implementing the proposed injection strategy in a feedback controller, which keeps the machine speed at 500 rpm with a constant load torque of 2 Nm. The injection ratio $k = i_{q3}/i_{q1}$ has been linearly changed from 0 to 1 in a 20 s time span and all the other components of $[i_{dq}]$ are kept to zero.

Consistently with the theoretical results, the optimal condition is obtained for $k \cong 0.19$, where the power losses are effectively reduced from an initial value of about 188 W to the minimum value of about 160 W.

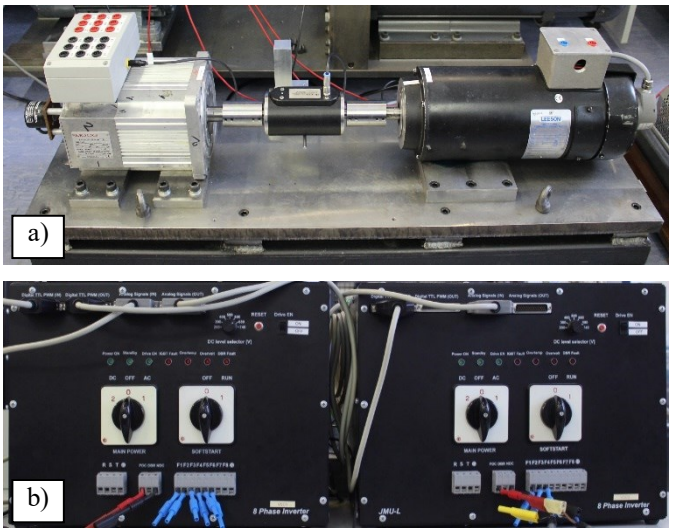


Fig. 13. Experimental test bench for the asymmetrical nine-phase drive: a) Nine-phase PMSM and dc brake; b) Multiphase inverters.

## B. Experimental Results

The experimental validation of the theoretical results has been performed using the nine-phase PMSM described in [23], whose windings have been properly rearranged to an asymmetrical configuration. The shaft of the PMSM has been coupled to a dc machine (used for loading) by a Datum Electronics M425 torque meter (Fig. 13a). The machine has been supplied using two custom-made multiphase inverters, based on Infineon FS50R12KE3 IGBT modules (Fig. 13b). They have a common dc-link, whose voltage is equal to 450 V and is supplied by a Sorensen SGI600/25 single quadrant dc-voltage source. The switching frequency of the inverter has been set to 5 kHz. The control algorithm has been implemented with a dSPACE ds1006 platform working at 10 kHz. An ADC board (ds2004) has been used to acquire the phase currents measured by the inverter's internal LEM sensors, while an incremental encoder board (ds3002) has provided the speed/position from the encoder. Additional measurements have been recorded using a Tektronix DPO/MSO 2014 oscilloscope, equipped with TCP0030A current probes.

The measured value of one induced back-EMF waveform (phase $a_1$) and the corresponding harmonic spectrum are depicted in Fig. 14. The magnitude spectrum is normalized by the fundamental harmonic, while the phase spectrum is shifted in order to obtain a phase of 90° for the fundamental component (i.e. in this way the phase $\varphi_1$ of the fundamental component of the corresponding flux $\lambda_{a_1} = \int_0^t e_{a_1}(\tau)\mathrm{d}\tau$ is set to zero).

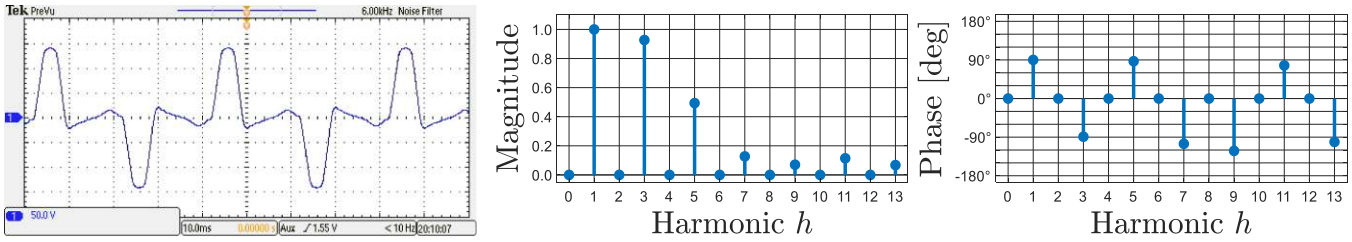


Fig. 14. PM induced back-EMF waveform (left, obtained at around 1500 rpm) and harmonic spectrum (right, normalized by the fundamental).

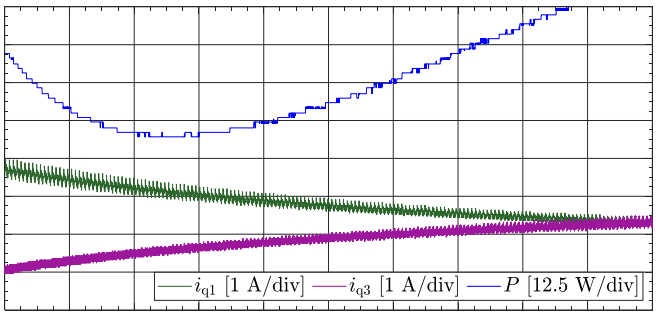


Fig. 15. Average losses ($P$), and quadrature currents ($i_{q1}$,$i_{q3}$) for a linearly varying injection ratio ($k = i_{q3}/i_{q1}$) in a 20 s time window (2 s/div).

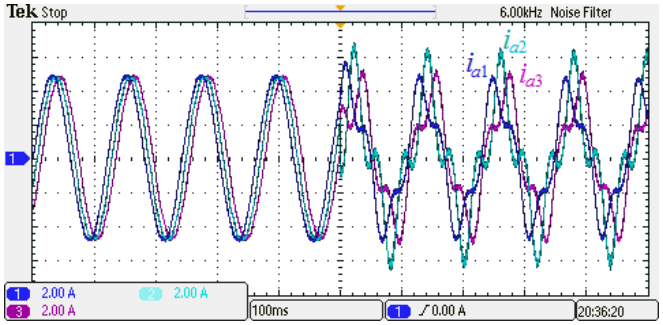


Fig. 16. Phase currents (multiplied by 4) without/with the optimal third harmonic injection.

The experiment follows the scenario described in the previous subsection: the $i_{q1}$ and $i_{q3}$ currents have been exploited for the torque development and the test has been performed by linearly varying the ratio $k = i_{q3}/i_{q1}$ in the interval [0; 1] during a time window of 20 s. The machine runs at a constant speed of 500 rpm with a load torque of about 2 Nm.

Fig. 15 shows the average stator power losses $P$ and the quadrature currents $i_{q1}$ and $i_{q3}$ (obtained by processing measured currents) during the testing interval. The resulting waveforms are very similar to the corresponding simulation results depicted in Fig. 12. The minimum dissipation is reached around 4.5 s; it corresponds to $k \cong 0.22$, which is reasonably close to the theoretical optimal ratio $k_{opt} \cong 0.19$ obtained from (21).

In Fig. 16 the $\{a_1, a_2, a_3\}$ current waveforms without and with the optimal third harmonic injection are shown. They have been obtained by step-changing the injection ratio $k$ from zero to the theoretical optimal value $k \cong 0.19$. As is evident, after an initial short transient, there is a good agreement with the corresponding theoretical current waveforms depicted in Fig. 3.

## VI. Conclusion

The paper presents a modelling approach and an optimal strategy to exploit a third harmonic current injection for the torque enhancement in multiphase isotropic PMSMs with non-sinusoidal back-EMFs.

The modelling approach is presented for a generic (i.e. asymmetrical, with an arbitrary angular shift) winding configuration and is based on the vector space decomposition (VSD) and rotational transformation. The torque developed by the machine can be expressed as a linear combination of the quadrature components of the currents space vectors linked to each harmonic contribution.

The choice of a proper Clarke's transformation matrix is crucial to select the desired harmonics, which can be effectively controlled. In a general case (and contrary to the symmetrical winding configurations) the transformation matrices are not unitary. This affects the power loss expression, which weights differently each current harmonic component. Moreover, when the machine's electrical equations are expressed using the transformed variables, the asymmetrical machine configuration usually leads to coupling among the different space vectors, which should be properly compensated in the current control.

Once the transformed set has been chosen, the proposed strategy is based on the choice of a constant current set in the multiple synchronous domain. This choice greatly simplifies the power loss expression, it allows to directly relate each current space vector to a given steady state harmonic injected into the phase currents, and it makes it possible to design the feedback controller via PI regulators and compensating actions. The strategy chooses a constant $i_{q1}$ (responsible for the fundamental currents) and a constant $i_{q3}$ (responsible for the third harmonic injection). Their ratio is computed in a way which minimizes the average winding losses for a given torque. This problem has an analytical solution which only depends on the magnitude of the PM induced fluxes and on the stator windings' disposition.

The strategy has been particularized for some specific asymmetrical configurations (including those where symmetrical winding is preferred, such as 9- and 15-phase) in order to highlight its properties. An experimental validation has also been performed using an asymmetrical nine-phase machine. Both the simulation and the experimental results are in a good agreement with the theoretical analysis.

## References


[1] E. Levi, "Multiphase electric machines for variable-speed applications," *IEEE Trans. Ind. Electron.*, vol. 55, no. 5, 2008.

[2] E. Levi, F. Barrero and M. J. Duran, "Multiphase machines and drives – revisited," *IEEE Trans. Ind. Electron.*, vol. 63, 2016.

[3] E. Levi, R. Bojoi, F. Profumo, H. A. Toliyat and S. Williamson, "Multiphase induction motor drives - a technology status review," *IET Electr. Power Appl.*, vol. 1, no. 4, 2007.

[4] M. Farshadnia, M. A. Masood Cheema, A. Pouramin, R. Dutta and J. E. Fletcher, "Design of optimal winding configurations for symmetrical multiphase concentrated-wound surface-mount PMSMs to achieve maximum torque density under current harmonic Injection," *IEEE Trans. Ind. Electron.*, vol. 65, no. 2, 2018.

[5] K. Wang, Z. Q. Zhu and G. Ombach, "Torque enhancement of surface-mounted permanent magnet machine using third-order harmonic," *IEEE Trans. Magnetics*, vol. 50, no. 3, 2014.

[6] K. Wang, Z. Y. Gu, Z. Q. Zhu and Z. Z. Wu, "Optimum injected harmonics into magnet shape in multiphase surface-mounted PM machine for maximum output torque," *IEEE Trans. Ind. Electron.*, vol. 64, no. 6, 2017.

[7] J. Wang, L. Zhou and R. Qu, "Harmonic current effect on torque density of a multiphase permanent magnet machine," *Int. Conf. Electric Mach. and Sys. ICEMS*, 2011.

[8] Z. Q. Zhu, K. Wang and G. Ombach, "Optimal magnet shaping with third order harmonic for maximum torque in SPM machines," *6th IET Conf. on Power Electron., Mach. and Drives PEMD*, 2012.

[9] L. Parsa and H. A. Toliyat, "Five-phase permanent magnet motor drives," *IEEE Trans. Ind. Appl.*, vol. 41, no. 1, 2005.

[10] L. Parsa and H. A. Toliyat, "Five-phase permanent magnet motor drives for ship propulsion applications," *Electr. Ship Tech. Symp. ESTS*, 2005.

P. J. McCleer, J. M. Bailey and J. S. Lawler, "Five phase trapezoidal back emf PM synchronous machines and drives," *Eur. Power Electron. and Appl. Conf. EPE*, 1991.

[12] K. Wang, Z. Y. Gu, C. Liu and Z. Q. Zhu, "Design and analysis of a five-phase SPM machine considering third harmonic current injection," *IEEE Trans. Energy Conv.*, vol. 33, no. 3, 2018.

[13] L. Parsa, N. Kim and H. A. Toliyat, "Field weakening operation of high torque density five-phase permanent magnet motor drives," *IEEE Int.*

*Electric Mach. and Drives Conf. IEMDC*, 2005.
[14] B. Aslan and E. Semail, "New 5-phase concentrated winding machine with bi-harmonic rotor for automotive application," *Int. Conf. Electric Mach. ICEM*, 2014.
[15] Y. Sui, P. Zheng, Y. Fan and J. Zhao, "Research on the vector control strategy of five-phase PMSM based on third-harmonic current injection," *IEEE Int. Electric Mach. and Drives Conf. IEMDC*, 2017.
[16] Z. Y. Gu, K. Wang, Z. Q. Zhu, Z. Z. Wu, C. Liu and R. W. Cao,"Torque improvement in five-phase unequal tooth SPM machine by injecting third harmonic current," *IEEE Trans. Vech. Techn.*, vol. 67, no. 1, 2018.
[17] J. Gong, H. Zahr, E. Semail, M. Trabelsi, B. Aslan and F. Scuiller, "Design considerations of five-phase machine with double p/3p polarity," *IEEE Trans. Energy Conv*, vol. 34, no. 1, 2019.
[18] Y. Hu, Z. Q. Zhu and M. Odavic, "Torque capability enhancement of dual three-phase PMSM drive with fifth and seventh current harmonics injection," *2016 XXII Int. Conf. on Electr. Mach. ICEM*, 2016.
[19] R. O. C. Lyra and T. A. Lipo, "Torque density improvement in a six-phase induction motor with third harmonic current injection," *IEEE Trans. Ind. Appl.*, vol. 38, no. 5, 2002.
[20] B. Stumberger, G. Stumberger, A. Hamler, M. Trlep, M. Jesenik and V. Gorican, "Increasing of output power capability in a six-phase flux-weakened permanent magnet synchronous motor with a third harmonic current injection," *IEEE Trans. Magnetics*, vol. 39, no. 5, 2003.
[21] K. Wang, J. Y. Zhang, Z. Y. Gu, H. Y. Sun and Z. Q. Zhu, "Torque improvement of dual three-phase permanent magnet machine using zero sequence components," *IEEE Trans. Magnetics*, vol. 53, no. 11, 2017.
[22] A. Cervone, M. Slunjski, E. Levi and G. Brando, "Optimal third-harmonic current injection for an asymmetrical nine-phase PMSM with non-sinusoidal back-EMF" *45th Ann. Conf. of IEEE Ind. Electron. Soc. IECON*, 2019
[23] M. Slunjski, M. Jones, E. Levi, "Analysis of a symmetrical nine-phase machine with highly non-sinusoidal back-EMF force," 44*th Ann. Conf. of IEEE Ind. Electron. Soc. IECON*, pp. 6229-6234, 2018.

**Andrea Cervone** (S'19) received the BSc and MSc degrees in Electrical Engineering at the University of Naples Federico II in 2014 and 2017, respectively. He is currently a PhD student in Electrical Engineering at the University of Naples Federico II. His research interests are mainly focused on multilevel converters and electrical drives.

**Marko Slunjski** (S'18) received the BSc and MSc degrees in Electrical Engineering from the University of Zagreb, Faculty of Electrical Engineering and Computing, Croatia in 2015 and 2017, respectively. Since July 2017, he has been with Liverpool John Moores University, Liverpool, U.K., where he is working toward the Ph.D. degree in electrical engineering. His main research interests are in the areas of power electronics and advanced variable speed multiphase drive systems.

**Emil Levi** (S'89, M'92, SM'99, F'09) received his MSc and the PhD degrees in Electrical Engineering from the University of Belgrade, Yugoslavia in 1986 and 1990, respectively. He joined Liverpool John Moores University, UK in May 1992 and is since September 2000 Professor of Electric Machines and Drives. He served as a Co-Editor-in-Chief of the IEEE Trans. on Industrial Electronics in the 2009-2013 period. Currently he is Editor-in-Chief of the IEEE Trans. on Industrial Electronics, Editor-in-Chief of the IET Electric Power Applications and an Editor of the IEEE Trans. on Energy Conversion. He is the recipient of the Cyril Veinott award of the IEEE Power and Energy Society for 2009 and the Best Paper award of the IEEE Trans. on Industrial Electronics for 2008. In 2014 he received the "Outstanding Achievement Award" from the European Power Electronics (EPE) Association and in 2018 the "Professor Istvan Nagy Award" from the Power Electronics and Motion Control (PEMC) Council.

**Gianluca Brando** received the MSs (cum laude) and PhD degrees in Electrical Engineering from the University of Naples Federico II, Italy, in 2000 and 2004. He was, from 2000 to 2012, a Postdoctoral Research Fellow in the Department of Electrical Engineering, University of Naples Federico II, Naples, Italy. Since 2012 he is assistant professor of Electrical Machines and Drives at the Department of Electrical Engineering and Information Technology, University of Naples Federico II. He is an author of several scientific papers published in international journals and conference proceedings. His research interests are focused on control strategies for renewable energy sources.